

Effects of R-parity violation in unpolarized top quark decay into polarized W-boson

Yi Min Nie, Chong Sheng Li*, Qiang Li, Jian Jun Liu and Jun Zhao

Department of Physics, Peking University, Beijing 100871, China

December 2, 2024

Abstract

We calculate one-loop R-parity violating corrections to the top quark decay into a bottom quark and a polarized W-gauge boson. The corrections are presented according to the total corrections, the longitudinal corrections and the transverse corrections, respectively. We compared our results with the $\mathcal{O}(\alpha_s)$ QCD corrections, the $\mathcal{O}(\alpha)$ electroweak (EW) and finite width corrections, and also the supersymmetric (SUSY) corrections with R-parity conservation, respectively.

PACS number: 14.80.Ly, 14.65.Ha, 12.60.Jv

Keywords: Radiative correction, Top quark decay, R-parity violation.

*csli@pku.edu.cn

1 Introduction

The top quark is the heaviest known fermion with a mass close to the scale of the electroweak(EW) symmetry breaking. Therefore the study of its properties and the possible deviations from standard model (SM) predictions can probe varies physics beyond the SM. The Tevatron run I has yielded relatively small numbers of top quark events. But the Tevatron run II can provide copious top quark events, and improve the precision of the top quark measurements, moreover, the CERN Large Hadron Collider (LHC) and the Next-generation Linear Collider (NLC) will serve as top quark factories, and these machines should be very useful to obtain the information of new physics through analyzing the properties of the top quark decay, especially the study of the polarized properties of the decay products will be a good probe of new physics.

The dominate decay mode of the top quark is $t \rightarrow bW^+$, where the W boson as a decay product is strongly polarized with three helicity contents: transverse plus, transverse minus and longitudinal. The recent measurement of the top quark mass is $m_t = 178.0 \pm 4.3$ GeV (world average) [1], which implies

$$\Gamma = 1.86 \text{ GeV} \text{ (including } \mathcal{O}(\alpha_s) \text{ QCD corrections),} \quad (1)$$

and the helicity of the W boson measured by CDF Collaborations [2] before the publication of [1] is

$$\Gamma_L/\Gamma = 0.91 \pm 0.37(\text{stat}) \pm 0.13(\text{syst}), \quad (2)$$

and

$$\Gamma_+/\Gamma = 0.11 \pm 0.15 \quad (\text{assuming } \Gamma_L/\Gamma = 0.7), \quad (3)$$

where Γ is the total width of $t \rightarrow bW^+$, Γ_L and Γ_+ are the longitudinal and the transverse-plus widths, respectively. Since the size of the longitudinal contribution encodes the physics of the spontaneous breaking of the electroweak symmetry, and the transverse-plus contribution vanishes at the Born-level, any sizable deviation from them may indicate obvious quantum effects or a non-SM (V+A) coupling in the weak $t \rightarrow b$ current transition. Therefore, the investigation of radiative corrections to the top decay into a polarized W boson may provide additional

information about the new physics, and there has been a great of interests from theorists. So far theoretical predictions of these observables reported in the literatures are summarized as follows: the QCD corrections to the top width are rather large in general. One-loop QCD corrections to tree-level width are -8.54% [3–8], one-loop electroweak corrections are $+1.54\%$ [3, 9, 10] and two-loop QCD corrections are approximate -2.05% [11] (-2.16% [12]), and the one-loop SUSY-QCD and SUSY-EW corrections are below 1% in magnitude for most of the parameter space [15]. As for the partial longitudinal and transverse rates, for the top quark mass $m_t = 175\text{GeV}$, the tree-level results are 0.703 for Γ_L/Γ , 0.297 for Γ_-/Γ and $\mathcal{O}(10^{-4})$ for Γ_+/Γ , respectively. In the SM, the $\mathcal{O}(\alpha_s)$ QCD corrections decrease the rate Γ_L/Γ by 1.06%, increase the rate Γ_-/Γ by 2.17% and the rate Γ_+/Γ reach mere 0.10% [13]. The electroweak and finite width corrections increase the rate Γ_L/Γ by 1.32%, increase the rate Γ_-/Γ by 2.06% and the rate Γ_+/Γ are only $\mathcal{O}(0.1\%)$ [14]. Beyond the SM, one-loop SUSY-QCD and SUSY-EW corrections to Γ_-/Γ and Γ_L/Γ are less than 1% in magnitude and tend to have opposite signs [15]. However, the R-parity violating SUSY contributions to $t \rightarrow bW^+$ have not been calculated so far. In this paper we will investigate the R-parity violating SUSY contributions to $t \rightarrow bW^+$, including the total corrections, the longitudinal corrections and the transverse corrections, respectively.

The most general superpotential of the minimal supersymmetric standard model (MSSM) consistent with the $SU(3) \times SU(2) \times U(1)$ symmetry and supersymmetry contains R-violating interactions, which are given by [16]

$$\mathcal{W}_R = \frac{1}{2}\lambda_{ijk}L_iL_jE_k^c + \lambda'_{ijk}\delta^{\alpha\beta}L_iQ_{j\alpha}D_{k\beta}^c + \frac{1}{2}\lambda''_{ijk}\varepsilon^{\alpha\beta\gamma}U_{i\alpha}^cD_{j\beta}^cD_{k\gamma}^c + \mu_iL_iH_2. \quad (4)$$

Here $L_i(Q_i)$ and $E_i(U_i, D_i)$ are, respectively, the left-handed lepton (quark) doublet and right-handed lepton (quark) singlet chiral superfields, and $H_{1,2}$ are the Higgs chiral superfields. The indices i, j, k denote generations and α, β and γ are the color indices, and the superscript c denotes charge conjugation. The λ and λ' are the coupling constants of L(lepton number)-violating interactions and λ'' those of B(baryon number)-violating interactions. The non-observation (so far) of the proton decay imposes very strong constraints on the product of L-violating and B-violating couplings. It is thus conventionally assumed in the phenomenological studies that only one type of these interactions (either L- or B-violating) exists. Some constraints on these

R-parity violating couplings have been obtained from various analysis of their phenomenological implications based on experiments. It is notable that the bounds on the couplings involving top quark are generally quite weak. As the large number of top quarks will be produced at the future colliders, these couplings may either manifest themselves, or stronger constraints on them can be established. For the purpose of our work, we will focus on the quantum effects of R-parity violating couplings involved λ_{ijk}'' and λ_{ijk}' in the top quark decay into polarized W^+ boson, respectively.

This paper is organized as follows. In the Sec.2 we present some formulas for our calculations, by which we can calculate the helicity amplitude of the top quark decays. In the Sec.3 we take a careful study on R-parity violating effects using the helicity method. In the Sec.4 we make a numerical analysis with drawing some conclusions for our calculations. The explicit expressions of the helicity amplitudes induced by the R-parity violating couplings are given in the Appendix.

2 Formalism

In order to make our paper self-constrained, we start with a brief description of the helicity amplitude method for performing the following calculations. The method breaks down the algebra of four-dimensional Dirac spinors and matrices into equivalent two-dimensional ones. In what follows we introduce the Weyl representation of Dirac spinors and matrices. In spherical coordinates the four-momemta can be written as

$$p^\mu = (E, |\vec{p}| \sin \theta \cos \varphi, |\vec{p}| \sin \theta \sin \varphi, |\vec{p}| \cos \theta), \quad (5)$$

with $E^2 - |\vec{p}|^2 = m^2$. The left-hand (L), right-hand (R) and longitudinal (0) polarization vectors for a spin-1 field are defined as [23]

$$\begin{aligned} \varepsilon_{(L)}^\mu &= \frac{e^{-i\phi}}{\sqrt{2}} (0, i \sin \phi + \cos \phi \cos \theta, -i \cos \phi + \sin \phi \cos \theta, -\sin \theta), \\ \varepsilon_{(R)}^\mu &= \frac{e^{i\phi}}{\sqrt{2}} (0, i \sin \phi - \cos \phi \cos \theta, -i \cos \phi - \sin \phi \cos \theta, \sin \theta), \\ \varepsilon_{(0)}^\mu &= \frac{1}{m} (|\vec{p}|, E \sin \theta \cos \phi, E \sin \theta \sin \phi, E \cos \theta). \end{aligned} \quad (6)$$

The above equations satisfy the identities $\varepsilon_{(R)}^\mu = -\varepsilon_{(L)}^{\mu*}$, $\varepsilon_{(0)}^\mu = \varepsilon_{(0)}^{\mu*}$, $p_\mu \varepsilon_{(h)}^\mu = 0$ and $\varepsilon_\mu^{(h)} \varepsilon_{(h')}^{\mu*} = -\delta_{hh'}$ for $h, h' = R, L$ or 0 . In the Weyl basis Dirac spinors have the following four component forms

$$\psi = \begin{pmatrix} \psi_+ \\ \psi_- \end{pmatrix}. \quad (7)$$

For fermions (with helicity $\lambda = \pm 1$),

$$\psi_\pm = \begin{cases} u_\pm^{(\lambda=1)} = \omega_\pm \chi_{1/2} \\ u_\pm^{(\lambda=-1)} = \omega_\mp \chi_{-1/2} \end{cases}, \quad (8)$$

and for anti-fermions (with helicity $\lambda = \pm 1$),

$$\psi_\pm = \begin{cases} v_\pm^{(\lambda=1)} = \pm \omega_\mp \chi_{-1/2} \\ v_\pm^{(\lambda=-1)} = \mp \omega_\pm \chi_{1/2} \end{cases}, \quad (9)$$

with $\omega_\pm = \sqrt{E \pm |\vec{p}|}$. The $\chi_{\lambda/2}$'s are eigenvectors of the helicity operator

$$h = \vec{p} \cdot \vec{\sigma}, \quad \hat{p} = \vec{p}/|\vec{p}|, \quad (10)$$

where $\sigma_{j=1,2,3}$ are the Pauli matrices. We use the top rest frame, and one can write down these eigenvectors with eigenvalue λ (for simplicity we take $\phi = 0$) as

$$\chi_{1/2} = \begin{pmatrix} \cos \frac{\theta}{2} \\ \sin \frac{\theta}{2} \end{pmatrix}, \quad \chi_{-1/2} = \begin{pmatrix} -\sin \frac{\theta}{2} \\ \cos \frac{\theta}{2} \end{pmatrix}, \quad (11)$$

where $\lambda = \pm 1$ are for "spin-up" and "spin-down", respectively. In the Weyl basis \not{p} takes the form

$$\not{p} = p_\mu \gamma^\mu \equiv \begin{pmatrix} 0 & \not{p}_+ \\ \not{p}_- & 0 \end{pmatrix} \equiv p_\mu \begin{pmatrix} 0 & \gamma_+^\mu \\ \gamma_-^\mu & 0 \end{pmatrix}, \quad (12)$$

where

$$\gamma_\pm^\mu = (1, \pm \vec{\sigma}). \quad (13)$$

According to the above discussions, in the top rest frame we can write down the following expressions:

$$\begin{aligned}
p_t^\mu &= (m_t, 0, 0, 0), \\
p_W^\mu &= (E_W, -|\vec{p}_W| \sin \theta, 0, -|\vec{p}_W| \cos \theta), \\
\varepsilon_{(+)}^\mu &= \frac{1}{\sqrt{2}}(0, \cos \theta, -i, -\sin \theta), \\
\varepsilon_{(0)}^\mu &= \frac{1}{M_W}(|\vec{p}_W|, -E_W \sin \theta, 0, -E_W \cos \theta), \\
\varepsilon_{(-)}^\mu &= -(\varepsilon_{(+)}^\mu)^*,
\end{aligned} \tag{14}$$

where p_t^μ and p_W^μ are the four-dimensional momenta of the top quark and W boson, $\varepsilon_{(+)}^\mu$, $\varepsilon_{(-)}^\mu$ and $\varepsilon_{(0)}^\mu$ denote the left-hand (L), right-hand (R) and longitudinal (0) polarization vectors of W boson, respectively. Moreover, E_W is the energy of the W boson and \vec{p}_b is the momentum of the bottom quark. They can be expressed as

$$E_W = \frac{m_t^2 + m_b^2 - M_W^2}{2m_t}, \tag{15}$$

$$|\vec{p}_b| = \frac{1}{2m_t} \sqrt{[(m_t + m_b)^2 - M_W^2][(m_t - m_b)^2 - M_W^2]}. \tag{16}$$

3 Calculations

3.1 Tree level results

The tree level amplitude, as shown in Fig.1(a), is given by

$$A_0 = \bar{u}(p_b) \gamma^\mu \left[\frac{-ig}{\sqrt{2}} \left(\frac{1 - \gamma_5}{2} \right) \right] u(p_t) \varepsilon_\mu(p_W), \tag{17}$$

where ε_μ is the polarization vector of W boson. According to the previous discussions in Section II, the corresponding helicity amplitude can be written as

$$A_0(\lambda_t, \lambda_b, \lambda_W) = \frac{-ig}{\sqrt{2}} u_-^\dagger(p_b, \lambda_b) \gamma_+^\mu u_-(p_t, \lambda_t) \varepsilon_\mu(p_W, \lambda_W).$$

According to Eq.(12), the spinor of the bottom quark is

$$u_-(\lambda_b = -1) = \omega_+(b)\chi_{-\frac{1}{2}}(b) = \sqrt{E_b + |\vec{p}_b|} \begin{pmatrix} -\sin \frac{\theta}{2} \\ \cos \frac{\theta}{2} \end{pmatrix}, \quad (18)$$

$$u_-(\lambda_b = +1) = \omega_-(b)\chi_{\frac{1}{2}}(b) = \sqrt{E_b - |\vec{p}_b|} \begin{pmatrix} \cos \frac{\theta}{2} \\ \sin \frac{\theta}{2} \end{pmatrix}, \quad (19)$$

where

$$E_b = \frac{m_t^2 + M_W^2 - m_b^2}{2m_t}.$$

And the spinors of the spin-down(up) top quark are shown as below, respectively,

$$u_-(\lambda_t = -1) = \omega_+(t)\chi_{-\frac{1}{2}}(t) = \sqrt{E_t} \begin{pmatrix} 0 \\ 1 \end{pmatrix}, \quad (20)$$

$$u_-(\lambda_t = +1) = \omega_-(t)\chi_{\frac{1}{2}}(t) = \sqrt{E_t} \begin{pmatrix} 1 \\ 0 \end{pmatrix}. \quad (21)$$

Thus the explicit expressions of the helicity amplitudes $A(\lambda_t, \lambda_b, \lambda_W)$ are given by

$$\begin{aligned} A_0(+, -, 0) &= \frac{ig}{\sqrt{2}M_W} \sqrt{(E_b + |\vec{p}_b|)E_t} (E_W + |\vec{p}_b|) \sin \frac{\theta}{2}, \\ A_0(+, -, -1) &= -ig \sqrt{(E_b + |\vec{p}_b|)E_t} \cos \frac{\theta}{2}, \\ A_0(+, -, +1) &= 0, \\ A_0(-, -, 0) &= \frac{-ig}{\sqrt{2}M_W} \sqrt{(E_b + |\vec{p}_b|)E_t} (E_W + |\vec{p}_b|) \cos \frac{\theta}{2}, \\ A_0(-, -, -1) &= -ig \sqrt{(E_b + |\vec{p}_b|)E_t} \sin \frac{\theta}{2}, \\ A_0(-, -, +1) &= 0. \\ A_0(+, +, 0) &= \frac{ig}{\sqrt{2}M_W} (E_W - |\vec{p}_b|) \sqrt{(E_b - |\vec{p}_b|)E_t} \cos \frac{\theta}{2}, \\ A_0(+, +, -1) &= 0, \\ A_0(+, +, +1) &= -ig \sqrt{(E_b - |\vec{p}_b|)E_t} \sin \frac{\theta}{2}, \\ A_0(-, +, 0) &= \frac{-ig}{\sqrt{2}M_W} (E_W - |\vec{p}_b|) \sqrt{(E_b - |\vec{p}_b|)E_t} \sin \frac{\theta}{2}, \\ A_0(-, +, -1) &= 0, \\ A_0(-, +, +1) &= -ig \sqrt{(E_b - |\vec{p}_b|)E_t} \cos \frac{\theta}{2}. \end{aligned}$$

In this paper we only consider the longitudinal width Γ_L or the transverse width Γ_T induced by the polarization of the W^+ , so we should sum the helicities of the top quark and the bottom quark. Using the previous results, the tree-level ratio of Γ_L and Γ_T is

$$\frac{\Gamma_L}{\Gamma_T} = \frac{\sum_{\lambda_t, \lambda_b} |A_0|^2(\lambda_t, \lambda_b, \lambda_W = 0)}{\sum_{\lambda_t, \lambda_b} |A_0|^2(\lambda_t, \lambda_b, \lambda_W = \pm 1)} = \frac{M_W^2 + 2|\vec{p}_b|^2 + 2\frac{E_W}{E_b}|\vec{p}_b|^2}{2M_W^2}. \quad (22)$$

If the mass of the bottom quark is neglected, Eq.(21) is simplified as

$$\frac{\Gamma_L}{\Gamma_T} = \frac{m_t^2}{2M_W^2}. \quad (23)$$

3.2 SUSY R-Parity violation corrections

The SUSY R-parity violation corrections arise from the Feynman diagrams shown in Fig1(b)-(c') and Fig (2)-(4), which consist of the vertex and self-energy diagrams. The Lagrangians involved the λ'' and λ' couplings are given by

$$\begin{aligned} \mathcal{L}_{UDD} &= -\lambda''_{ijk} \varepsilon_{\alpha\beta\gamma} [(\tilde{d}_R^{kr})^* \bar{u}_R^{i\alpha} (d_R^{j\beta})^c + \frac{1}{2} (\tilde{u}_R^{i\alpha})^* \bar{d}_R^{j\beta} (d_R^{k\gamma})^c] + h.c., \\ \mathcal{L}_{LQD} &= -\lambda'_{ijk} (\tilde{d}_{kR}^* \bar{v}_i^c P_L d_j - \tilde{d}_{kR}^* \bar{l}_i^c P_L u_j + \tilde{d}_{jL} \bar{d}_i^k P_L v_i \\ &\quad - \tilde{u}_{jL} \bar{d}_i^k P_L l_i + \tilde{v}_i \bar{d}_i^k P_L d_j - \tilde{l}_{iL} \bar{d}_i^k P_L u_j) + h.c.. \end{aligned} \quad (24)$$

Note that $\lambda''_{ijk} = -\lambda''_{ikj}$. When we consider the one-loop SUSY R-parity violation corrections, the renormalized amplitude can be written as

$$A^{ren} = A^0 + \delta A, \quad (25)$$

$$\delta A \equiv A^v + A^c, \quad (26)$$

where A^v and A^c are the vertex corrections and the counterterms, respectively.

- **The corrections from the λ'' couplings**

Calculating the diagrams in Fig.1 (b) and (c), we can get the explicit expressions of the vertex corrections as following:

$$A_1^v = \sum_{j,k=1}^3 \sum_{m=1}^2 \left\{ \frac{igX}{8\sqrt{2}\pi^2} \bar{u}(p_b) \gamma^\mu P_R u(p_t) \varepsilon_\mu(p_W) C_0(m_t^2, m_b^2, M_W^2, m_{d_j}^2, m_{u_j}^2, m_{\tilde{d}_{k,m}}^2) \right\}, \quad (27)$$

$$\begin{aligned} A_2^v &= \sum_{j,k=1}^3 \sum_{m,n=1}^2 \left\{ \frac{igY}{16\sqrt{2}\pi^2} [m_t \bar{u}(p_b) P_L u(p_t) C_\mu \varepsilon^\mu(p_W) \right. \\ &\quad \left. + 2\bar{u}(p_b) P_L \gamma^\mu C_{\mu\nu} \varepsilon^\nu(p_W) u(p_t)] (m_t^2, m_b^2, M_W^2, m_{d_j}^2, m_{\tilde{u}_{k,n}}^2, m_{\tilde{d}_{k,m}}^2) \right\}, \end{aligned} \quad (28)$$

with

$$\begin{aligned} X &= \lambda''_{3jk} \lambda''_{j3k} |R_{m2}^{\tilde{d}_k}|^2 m_{u_j} m_{d_j}, \\ Y &= -\lambda''_{3jk} \lambda''_{kj3} R_{n1}^{\tilde{u}_k} R_{n2}^{\tilde{u}_k} R_{m1}^{\tilde{d}_k} R_{m2}^{\tilde{d}_k}, \end{aligned}$$

where C_0 , C_μ and $C_{\mu\nu}$ are the three-point integrals, which are defined similar to [17] except that we take internal masses squared as arguments [18]. $m_{\tilde{u}_k(\tilde{d}_k)_{1,2}}$ ($k = 1, 2, 3$) are the squark masses, and $R^{\tilde{u}_k(\tilde{d}_k)}$ are 2×2 matrix, which are defined to transform the squark current eigenstates to the mass eigenstates.

The corresponding helicity amplitudes are

$$\begin{aligned} A_1^v(\lambda_t, \lambda_b, \lambda_W) &= \sum_{j,k=1}^3 \sum_{m=1}^2 \left\{ \frac{igX}{8\sqrt{2}\pi^2} u_+^\dagger(p_b, \lambda_b) \gamma_-^\mu u_+(p_t, \lambda_t) \varepsilon_\mu(p_W, \lambda_W) \right. \\ &\quad \left. \times C_0(m_t^2, m_b^2, M_W^2, m_{d_j}^2, m_{u_j}^2, m_{\tilde{d}_{k,m}}^2) \right\}, \end{aligned} \quad (29)$$

$$\begin{aligned} A_2^v(\lambda_t, \lambda_b, \lambda_W) &= \sum_{j,k=1}^3 \sum_{m,n=1}^2 \left\{ \frac{igY}{16\sqrt{2}\pi^2} [m_t u_-^\dagger(p_b, \lambda_b) u_-(p_t, \lambda_t) C_\mu \varepsilon^\mu(p_W, \lambda_W) \right. \\ &\quad \left. + 2u_+^\dagger(p_b, \lambda_b) \gamma_-^\mu u_+(p_t, \lambda_t) C_{\mu\nu} \varepsilon^\nu(p_W, \lambda_W)] (m_t^2, m_b^2, M_W^2, m_{d_j}^2, m_{\tilde{u}_{k,n}}^2, m_{\tilde{d}_{k,m}}^2) \right\}, \end{aligned} \quad (30)$$

the explicit expressions of which are shown in the Appendix.

The counterterm A^c can be expressed as

$$A^c = \left(\frac{1}{2} \delta Z_{L1}^t + \frac{1}{2} \delta Z_{L1}^b \right) A^0, \quad (31)$$

where $\delta Z_{L1}^t, \delta Z_{L1}^b$ are the renormalization constants, which are fixed by the on-shell renormalization scheme [19] and can be got from the calculations of the self-energy diagrams in Fig.2:

$$\delta Z_{L1}^t = - \sum_{j,k=1}^3 \sum_{m=1}^2 \left\{ \frac{im_t^2}{8\pi^2} |\lambda''_{3jk}|^2 |R_{m2}^{\tilde{d}_k}|^2 B'_1(p_t^2, m_{d_j}^2, m_{\tilde{d}_{k,m}}^2) \right\}, \quad (32)$$

$$\begin{aligned} \delta Z_{L1}^b &= - \sum_{i,k=1}^3 \sum_{m=1}^2 \left\{ \frac{im_b^2}{8\pi^2} |\lambda''_{i3k}|^2 |R_{m2}^{\tilde{d}_k}|^2 B'_1(m_b^2, m_{u_i}^2, m_{\tilde{d}_{k,m}}^2) \right. \\ &\quad \left. + \frac{im_b^2}{32\pi^2} |\lambda''_{i3k}|^2 |R_{m2}^{\tilde{u}_i}|^2 B'_1(m_b^2, m_{\tilde{u}_{i,m}}^2, m_{d_k}^2) \right\}, \end{aligned} \quad (33)$$

where $B'_1 = \partial B_1 / \partial p^2$, and B_1 is the two-point integral [18].

The one-loop SUSY R-parity violation corrections to the decay width are given by

$$\delta\Gamma_{\lambda_W} = 2\text{Re} \left\{ \frac{1}{2} \sum_{\lambda_t, \lambda_b} A^{(0)\dagger}(\lambda_t, \lambda_b, \lambda_W) \delta A(\lambda_t, \lambda_b, \lambda_W) \right\} \cdot PS ,$$

where $\lambda_W = (L, +, -)$, and PS is given by

$$PS = \frac{1}{16\pi m_t^3} \sqrt{[m_t^2 - (M_W + m_b)^2][m_t^2 - (M_W - m_b)^2]} . \quad (34)$$

The ratios $\delta\hat{\Gamma}_{\lambda_W} = \delta\Gamma_{\lambda_W} / \Gamma_0(\lambda_W = L, +, -)$ are then given by

$$\begin{aligned} \delta\hat{\Gamma}_L &= \sum_{j,k=1}^3 \sum_{m,n=1}^2 \left\{ \frac{M_W^2}{m_t[(3m_W^2 + 2|\vec{p}_b|^2)E_b + 2E_W|\vec{p}_b|^2]} \times \right. \\ &\quad \left\{ \frac{m_t m_b}{4\pi^2} [-X C_0(m_t^2, m_b^2, M_W^2, m_{d_j}^2, m_{u_j}^2, m_{\tilde{d}_{k,m}}^2) \right. \\ &\quad \left. + \frac{m_t^2}{M_W^2} |\vec{p}_b|^2 Y(C_{12} + C_{22})(m_t^2, m_b^2, M_W^2, m_{d_j}^2, m_{\tilde{u}_{k,n}}^2, m_{\tilde{d}_{k,m}}^2)] + \right. \\ &\quad \left. \frac{m_t[(3M_W^2 + 2|\vec{p}_b|^2)E_b + 2E_W|\vec{p}_b|^2]}{M_W^2} (\delta Z_{L1}^t + \delta Z_{L1}^b) \right\} \right\} \end{aligned} \quad (35)$$

$$\begin{aligned} \delta\hat{\Gamma}_- &= \sum_{j,k=1}^3 \sum_{m,n=1}^2 \left\{ \frac{M_W^2}{[(3m_W^2 + 2|\vec{p}_b|^2)E_b + 2E_W|\vec{p}_b|^2]} \times \right. \\ &\quad \left\{ (E_b + |\vec{p}_b|)(\delta Z_{L1}^t + \delta Z_{L1}^b) + \frac{m_b}{4\pi^2} [X C_0(m_t^2, m_b^2, M_W^2, m_{d_j}^2, m_{u_j}^2, m_{\tilde{d}_{k,m}}^2) \right. \\ &\quad \left. + Y C_{24}(m_t^2, m_b^2, M_W^2, m_{d_j}^2, m_{\tilde{u}_{k,n}}^2, m_{\tilde{d}_{k,m}}^2)] \right\} \right\}, \end{aligned} \quad (36)$$

$$\begin{aligned} \delta\hat{\Gamma}_+ &= \sum_{j,k=1}^3 \sum_{m,n=1}^2 \left\{ \frac{M_W^2}{[(3m_W^2 + 2|\vec{p}_b|^2)E_b + 2E_W|\vec{p}_b|^2]} \times \right. \\ &\quad \left\{ (E_b - |\vec{p}_b|)(\delta Z_{L1}^t + \delta Z_{L1}^b) + \frac{m_b}{4\pi^2} [X C_0(m_t^2, m_b^2, M_W^2, m_{d_j}^2, m_{u_j}^2, m_{\tilde{d}_{k,m}}^2) \right. \\ &\quad \left. + Y C_{24}(m_t^2, m_b^2, M_W^2, m_{d_j}^2, m_{\tilde{u}_{k,n}}^2, m_{\tilde{d}_{k,m}}^2)] \right\} \right\}. \end{aligned} \quad (37)$$

• The corrections from the λ' couplings

In the case of λ' , the results can be got in the same way, and we show the corrections as

following:

$$\begin{aligned}
\delta\Gamma_L &= \sum_{i,k=1}^3 \sum_{m=1}^2 \left\{ \frac{(E_b + |\vec{p}_b|)^2 (E_b + |\vec{p}_b|) E_t}{2m_W^2} (\delta Z_{L2}^t + \delta Z_{L2}^b) \right. \\
&+ \frac{(E_b + |\vec{p}_b|) |\vec{p}_b| m_b m_t^2}{8\pi^2 M_W} |\lambda'_{i3k}|^2 |R_{m1}^{\tilde{l}_i}|^2 C_{12}(m_t^2, m_b^2, M_W^2, m_{\tilde{d}_{k,m}}^2, 0, m_{l_i}^2) \\
&- \frac{(E_b + |\vec{p}_b|) (E_W + |\vec{p}_b|) m_t}{16\pi^2 M_W} |\lambda'_{i3k}|^2 |R_{m2}^{\tilde{d}_k}|^2 [(E_W + |\vec{p}_b|) |\vec{p}_b| C_{11} + \frac{m_t E_W (E_W + |\vec{p}_b|)}{M_W} C_{12} \\
&- M_W (E_W + |\vec{p}_b|) C_{12} - \frac{(1-Z)(E_W + |\vec{p}_b|)}{M_W} C_{24} + \frac{|\vec{p}_b| m_t (E_W + |\vec{p}_b|)}{M_W} (C_{22} - C_{23}) \\
&\left. - \frac{|\vec{p}_b| m_t^2}{M_W} C_{22}] (m_t^2, m_b^2, M_W^2, m_{\tilde{d}_{k,m}}^2, 0, m_{l_i}^2) \right\}, \quad (38)
\end{aligned}$$

$$\begin{aligned}
\delta\Gamma_- &= \sum_{i,k=1}^3 \sum_{m=1}^2 \left\{ \frac{(E_b + |\vec{p}_b|) E_t}{2} (\delta Z_{L2}^t + \delta Z_{L2}^b) + \frac{(E_b + |\vec{p}_b|) E_t}{8\pi^2} |\lambda'_{i3k}|^2 |R_{m2}^{\tilde{d}_k}|^2 [M_W^2 C_{11} \right. \\
&+ 2(1-Z) + (m_t E_W - M_W^2) C_{12}] (m_t^2, m_b^2, M_W^2, m_{\tilde{d}_{k,m}}^2, 0, m_{l_i}^2) \left. \right\}, \quad (39)
\end{aligned}$$

$$\begin{aligned}
\delta\Gamma_+ &= \sum_{i,k=1}^3 \sum_{m=1}^2 \left\{ \frac{(E_b - |\vec{p}_b|) E_t}{2} (\delta Z_{L2}^t + \delta Z_{L2}^b) + \frac{(E_b + |\vec{p}_b|) E_t}{8\pi^2} |\lambda'_{i3k}|^2 |R_{m2}^{\tilde{d}_k}|^2 \times \right. \\
&[M_W^2 C_{11} + 2(1-Z) + (m_t E_W - M_W^2) C_{12}] (m_t^2, m_b^2, M_W^2, m_{\tilde{d}_{k,m}}^2, 0, m_{l_i}^2) \left. \right\} \quad (40)
\end{aligned}$$

with

$$Z = [4C_{24} + M_W^2 C_{21} + m_b^2 C_{22} + 2(m_t E_W - M_W^2) C_{23}] (m_t^2, m_b^2, M_W^2, m_{\tilde{d}_{k,m}}^2, 0, m_{l_i}^2),$$

where $\delta Z_{L2}^t, \delta Z_{L2}^b$ are the renormalization constants, which can be got from the calculations of the self-energy diagrams in Fig.3-4:

$$\begin{aligned}
\delta Z_{L2}^t &= - \sum_{i,k=1}^3 \sum_{m=1}^2 \left\{ \frac{m_t^2}{16\pi^2} |\lambda'_{i3k}|^2 \times \right. \\
&\left. [|R_{m1}^{\tilde{l}_i}|^2 B'_1(m_t^2, m_{\tilde{l}_{i,m}}^2, m_{d_k}^2) + |R_{m2}^{\tilde{d}_k}|^2 B'_1(m_t^2, m_{\tilde{d}_{k,m}}^2, m_{l_i}^2)] \right\}, \quad (41)
\end{aligned}$$

$$\begin{aligned}
\delta Z_{L2}^b &= - \sum_{i,j,k=1}^3 \sum_{m=1}^2 \left\{ \frac{m_t^2}{16\pi^2} |\lambda'_{ij3}|^2 \times \right. \\
&[|R_{m1}^{\tilde{d}_j}|^2 B'_1(m_b^2, 0, m_{\tilde{d}_{j,m}}^2) \\
&+ |R_{m1}^{\tilde{u}_j}|^2 B'_1(m_b^2, m_{l_i}^2, m_{\tilde{u}_{j,m}}^2) + |R_{m1}^{\tilde{l}_i}|^2 B'_1(m_b^2, m_{\tilde{l}_{i,m}}^2, m_{u_j}^2)] \\
&\left. + |\lambda'_{i3k}|^2 [B'_1(m_b^2, 0, m_{d_k}^2) + |R_{m1}^{\tilde{l}_i}|^2 B'_1(m_b^2, 0, m_{\tilde{d}_{k,m}}^2)] \right\}. \quad (42)
\end{aligned}$$

4 Numerical Results and Conclusions

We now present some numerical results for the R-parity violation effects in the top quark decay into polarized W boson. In our numerical calculations the SM parameters were taken to be $\alpha_{ew} = 1/128.8$, $m_W = 80.419\text{GeV}$, $m_t = 178.0\text{GeV}$, $m_Z = 91.1882\text{GeV}$ and $m_b(m_b) = 4.25\text{GeV}$ [20].

The relevant SUSY parameters are determined as following:

(i) For the parameters $m_{\tilde{Q},\tilde{U},\tilde{D}}^2$ and $A_{t,b}$ in squark mass matrices

$$M_{\tilde{q}}^2 = \begin{pmatrix} M_{LL}^2 & m_q M_{LR} \\ m_q M_{RL} & M_{RR}^2 \end{pmatrix} \quad (43)$$

with

$$\begin{aligned} M_{LL}^2 &= m_{\tilde{Q}}^2 + m_q^2 + m_Z^2 \cos 2\beta (I_q^{3L} - e_q \sin^2 \theta_W), \\ M_{RR}^2 &= m_{\tilde{U},\tilde{D}}^2 + m_q^2 + m_Z^2 \cos 2\beta e_q \sin^2 \theta_W, \\ M_{LR} = M_{RL} &= \begin{pmatrix} A_t - \mu \cot \beta & (\tilde{q} = \tilde{t}) \\ A_b - \mu \tan \beta & (\tilde{q} = \tilde{b}) \end{pmatrix}, \end{aligned} \quad (44)$$

we used $m_{\tilde{t}_1}$, $A_t = A_b, \tan \beta$ and μ as the input parameters. To simplify the calculations we assumed $M_{\tilde{Q}} = M_{\tilde{U}} = M_{\tilde{D}}$, $m_{\tilde{d}_{1,2}} = m_{\tilde{s}_{1,2}} = m_{\tilde{b}_1} + 300\text{GeV}$, and $m_{\tilde{u}_{1,2}} = m_{\tilde{c}_{1,2}} = m_{\tilde{t}_1} + 300\text{GeV}$. Such assuming of the relation between the squark masses is done merely for simplicity, and actually, our numerical results are not sensitive to the squark masses of the first and second generation.

(ii) According to the experimental upper bound on the couplings in the R-parity violating interaction [21], we take the relevant R-parity violating parameters as $|\lambda''_{132}| = 1.00$, $|\lambda''_{313}| = 0.0026$, $|\lambda''_{323}| = 0.96$, $|\lambda'_{132}| = 0.5$, $|\lambda'_{323}| = 0.9$.

In the numerical calculation we find that the contributions induced by λ' couplings are rather small, and they only reach $\mathcal{O}(10^{-4})$. So we only discuss the effects induced by λ'' below. In most of the previous studies, the bottom quark mass was neglected, and $\Gamma_+ = 0$. In this paper we keep the bottom quark mass, and one has $\Gamma_+ \neq 0$. But the results for transverse-plus rate $\delta\Gamma_+/\Gamma_+^0$ are very small, which are around $\mathcal{O}(10^{-6})$, so we do not show them in the curves. The other results are shown in Fig.5-13.

Fig.5 shows the dependence of the total corrections $\delta\Gamma/\Gamma_0$ on $m_{\tilde{t}_1}$, assuming $\tan\beta = 40$, $\mu = 300, 500$ and 600GeV , respectively. One finds that the total corrections $\delta\Gamma/\Gamma_0$ increase with decreasing $m_{\tilde{t}_1}$, and increase with increasing μ . They can reach about 4.0%, when $m_{\tilde{t}_1} = 150\text{GeV}$ and $\mu = 600\text{GeV}$. Comparing with the results in MSSM with R-conservation reported in Ref. [15], these corrections are rather large and remarkable.

Fig.6 gives the total corrections $\delta\Gamma/\Gamma_0$ as a function of μ for $m_{\tilde{t}_1} = 150\text{GeV}$, $\tan\beta = 4$ and 40, respectively. It should be noted that the magnitude of μ below 200GeV have been ruled out by LEP II [22]. As shown in this figure, we will not consider these areas. We find that the corrections increase with increasing μ when $\mu > 0$, and the two curves have opposite trends when $\mu < 0$.

In Fig.7 we show the total corrections $\delta\Gamma/\Gamma_0$ as a function of $\tan\beta$ for $m_{\tilde{t}_1} = 150\text{GeV}$, $\mu = -600$ and 200GeV , respectively. We find that these corrections are not sensitive to $\tan\beta$ for the smaller value of $|\mu|$ ($|\mu| = 200\text{GeV}$), and sensitive to $\tan\beta$ for the larger values of $|\mu|$ ($|\mu| = 600\text{GeV}$), these features also can be seen from Fig.6.

Fig.8 presents the dependence of the longitudinal corrections $\delta\Gamma_L/\Gamma_L^0$ on $m_{\tilde{t}_1}$, assuming $\mu = 300\text{GeV}$, $\tan\beta = 4$ and 40, respectively. We find that these corrections increase with decreasing $m_{\tilde{t}_1}$, and the longitudinal corrections are rather large, which can reach about 3%. From this figure one can see that the main contributions to the corrections to $\delta\Gamma/\Gamma_0$ come from the longitudinal corrections.

Fig.9 shows the longitudinal corrections $\delta\Gamma_L/\Gamma_L^0$ as a function of $\tan\beta$, for $m_{\tilde{t}_1} = 150\text{GeV}$, $\mu = -600$ and 200GeV , respectively. From this figure, one can see that the corrections are not sensitive to $\tan\beta$. Comparing with Fig.6, these corrections are plus when $\mu > 0$ and minus when $\mu < 0$.

Fig.10 presents the dependence of the longitudinal corrections $\delta\Gamma_L/\Gamma_L^0$ on μ , assuming $m_{\tilde{t}_1} = 150\text{GeV}$, $\tan\beta = 4$ and 40, respectively. Note that the areas of $|\mu| < 200\text{GeV}$ has been ruled out by LEP II. We can see that the magnitudes of these corrections increase with increasing $|\mu|$.

The remainder of the figures show the transverse-plus $\delta\Gamma_-/\Gamma_-^0$ as the functions of $m_{\tilde{t}_1}$, μ and $\tan\beta$, respectively. From Fig.11-13 we can see that the magnitudes of the corrections arising from the λ'' couplings are smaller, which only got 0.4%. However, it is still important for the

precise measurements of the helicity content of the W gauge boson in top quark decays in the future experiments.

To summarize, in general the corrections induced by λ' couplings are negligibly small, but the corrections induced by λ'' couplings may be important. Especially, the total corrections $\delta\Gamma/\Gamma_0$ induced by the R-parity violation couplings λ'' can reach about 4%, which are smaller than the $\mathcal{O}(\alpha_s)$ radiative corrections [13], but are comparable with the corresponding results in MSSM with R-parity conservation [15]. In addition, The longitudinal corrections can reach about 3%, which are still smaller than the results of the $\mathcal{O}(\alpha_s)$ QCD corrections [13], but larger than both of the $\mathcal{O}(\alpha)$ EW and finite width corrections [14] and the SUSY corrections with R-parity conservation [15]. The magnitudes of the corrections to the transverse-minus are about 0.3%, which are comparable with the results of [15] with R-parity conservations, but are smaller than both of the $\mathcal{O}(\alpha_s)$ QCD corrections and the $\mathcal{O}(\alpha)$ EW and finite width corrections. The corrections to the transverse-minus and the transverse-plus are too small to be observed, while the total and longitudinal corrections induced by λ'' couplings may be observable in the precise measurements in top quark decays in the future experiments; at least, interesting new constraints on the R-parity violation couplings can be established.

Acknowledgments

This work is supported in part by the National Natural Science Foundation of China and the Specialized Research Fund for the Doctoral Program of Higher Education.

Appendix: Helicity Amplitudes

(1) The explicit expressions of the helicity amplitudes of A_1^v and A_2^v in the case of $\lambda_b = -1$ are

$$\begin{aligned}
A_1^v(+,-,0) &= \frac{ig}{8\sqrt{2}\pi^2} \frac{X}{M_W} \sqrt{(E_b - |\vec{p}_b|)E_t} (|\vec{p}_b| - E_W) \sin \frac{\theta}{2} C_0, \\
A_1^v(+,-,-1) &= \frac{-ig}{8\pi^2} X \sqrt{(E_b - |\vec{p}_b|)E_t} \cos \frac{\theta}{2} C_0, \\
A_1^v(+,-,+1) &= 0, \\
A_1^v(-,-,0) &= \frac{-ig}{8\sqrt{2}\pi^2} \frac{X}{M_W} \sqrt{(E_b - |\vec{p}_b|)E_t} (|\vec{p}_b| - E_W) \cos \frac{\theta}{2} C_0, \\
A_1^v(-,-,-1) &= \frac{-ig}{8\pi^2} X \sqrt{(E_b - |\vec{p}_b|)E_t} \sin \frac{\theta}{2} C_0, \\
A_1^v(-,-,+1) &= 0, \\
A_2^v(+,-,0) &= \frac{ig}{8\sqrt{2}\pi^2} Y \sqrt{(E_b - |\vec{p}_b|)E_t} \sin \frac{\theta}{2} \times \\
&\quad \left\{ -\frac{m_t^2}{M_W} |\vec{p}_b| (C_{12} + C_{22}) + \frac{E_W - |\vec{p}_b|}{M_W} C_{24} + \frac{m_t}{M_W} (E_W - |\vec{p}_b|) |\vec{p}_b| (C_{22} - C_{23}) \right\}, \\
A_2^v(+,-,-1) &= \frac{-ig}{8\pi^2} \sqrt{(E_b - |\vec{p}_b|)E_t} \cos \frac{\theta}{2} C_{24}, \\
A_2^v(+,-,+1) &= 0, \\
A_2^v(-,-,0) &= \frac{-ig}{8\sqrt{2}\pi^2} Y \sqrt{(E_b - |\vec{p}_b|)E_t} \cos \frac{\theta}{2} \times \\
&\quad \left\{ -\frac{m_t^2}{M_W} |\vec{p}_b| (C_{12} + C_{22}) + \frac{E_W - |\vec{p}_b|}{M_W} C_{24} + \frac{m_t}{M_W} |\vec{p}_b| (E_W - |\vec{p}_b|) (C_{22} - C_{23}) \right\}, \\
A_2^v(+,-,-1) &= \frac{-ig}{8\pi^2} \sqrt{(E_b - |\vec{p}_b|)E_t} \sin \frac{\theta}{2} C_{24}, \\
A_2^v(-,-,+1) &= 0.
\end{aligned}$$

(2) The explicit expressions of the helicity amplitudes of A_1^v and A_2^v in the case of $\lambda_b = +1$ are

$$\begin{aligned}
A_1^v(+,+,0) &= \frac{ig}{8\sqrt{2}\pi^2} X \sqrt{(E_b + |\vec{p}_b|)E_t} \frac{E_W + |\vec{p}_b|}{M_W} \cos \frac{\theta}{2} C_0, \\
A_1^v(+,+, -1) &= 0, \\
A_1^v(+,+, +1) &= \frac{-ig}{8\pi^2} X \sqrt{(E_b + |\vec{p}_b|)E_t} \sin \frac{\theta}{2} C_0, \\
A_1^v(-,+,0) &= \frac{-ig}{8\sqrt{2}\pi^2} X \sqrt{(E_b + |\vec{p}_b|)E_t} \frac{E_W + |\vec{p}_b|}{M_W} \sin \frac{\theta}{2} C_0, \\
A_1^v(-,+, -1) &= 0, \\
A_1^v(-,+, +1) &= \frac{-ig}{8\pi^2} X \sqrt{(E_b + |\vec{p}_b|)E_t} \cos \frac{\theta}{2} C_0,
\end{aligned}$$

$$\begin{aligned}
A_2^v(+, +, 0) &= \frac{ig}{8\sqrt{2}\pi^2} Y \sqrt{(E_b + |\vec{p}_b|)E_t} \cos \frac{\theta}{2} \times \\
\left\{ -\frac{m_t^2}{M_W^2} |\vec{p}_b| (C_{12} + C_{22}) + \frac{E_W + |\vec{p}_b|}{M_W} C_{24} + \frac{m_t}{M_W} |\vec{p}_b| (E_W + |\vec{p}_b|) (C_{22} - C_{23}) \right\}, \\
A_2^v(+, +, -1) &= 0, \\
A_2^v(+, +, +1) &= \frac{-ig}{8\pi^2} Y \sqrt{(E_b + |\vec{p}_b|)E_t} \sin \frac{\theta}{2} C_{24}, \\
A_2^v(-, +, 0) &= \frac{-ig}{8\sqrt{2}\pi^2} Y \sqrt{(E_b + |\vec{p}_b|)E_t} \sin \frac{\theta}{2} \times \\
\left\{ -\frac{m_t^2}{M_W^2} |\vec{p}_b| (C_{12} + C_{22}) + \frac{E_W + |\vec{p}_b|}{M_W} C_{24} + \frac{m_t}{M_W} |\vec{p}_b| (E_W + |\vec{p}_b|) (C_{22} - C_{23}) \right\}, \\
A_2^v(-, +, -1) &= 0, \\
A_2^v(-, +, +1) &= \frac{-ig}{8\pi^2} Y \sqrt{(E_b + |\vec{p}_b|)E_t} \cos \frac{\theta}{2} C_{24}.
\end{aligned}$$

References

- [1] D0 Collaboration, Nature 429, 638 (2004)
- [2] CDF Collaboration, T.Affolder et al. Phys. Rev. Lett.84, 216(2000)
- [3] A. Denner and T. Sack, Nucl. Phys. B358, 46 (1991)
- [4] J. Liu and Y.-P. Yao, Int. J. Mod. Phys. A6, 4925 (1991)
- [5] A. Czarnecki, Phys. Lett. B252, 467 (1990)
- [6] C. S. Li, R. J. Oakes and T. C. Yuan, Phys. Rev. D43, 3759(1991)
- [7] M. Jeżabek and J. H. Kühn, Nucl. Phys. B314, 1(1989)
- [8] A. Ghinculov and Y. P. Yao, Mod. Phys. Lett. A15, 925(2000)
- [9] G. Eilam, R.R. Mendel, R. Migneron and A. Soni, Phys. Rev. Lett. 66, 3105(1991)
- [10] A. Barroso, L. Brücher and R. Santos, Phys. Rev. D62, 096003(2000)
- [11] A. Czarnecki and K. Melnikov, Nucl. Phys. B544, 520(1999)
- [12] K.G. Chetyrkin, R. Harlander, T. Seidensticker and M. Steinhauser, Phys. Rev. D60, 114015(1999)
- [13] M. Fischer, S. Groote, J.G. Körner and M.C. Mauser, Phys. Lett. B451, 406 (1999); Phys. Rev. D63, 031501(R)(2001); Phys. Rev. D63, 054036 (2002)
- [14] M. Fischer, S. Groote, J. G. Körner and M. C. Mauser, Phys. Rev. D67, 091501 (R)(2003)
- [15] J. J. Cao, R. J. Oakes, F. Wang and J. M. Yang, Phys. Rev. D68, 054019 (2003)
- [16] S. Weinberg, Phys. Rev. D26, 287(1982); N.Sakai, T.Yanagida, Nucl. Phys. B197, 133(1982)
- [17] G 't Hooft and M. Veltman, Nucl. Phys. B44, 189 (1972)
- [18] A.Denner, Fortschr. Phys.41, 4 (1993)

- [19] A. Sirlin, Phys. Rev. D22, 971 (1980); W. J. Marciano and A. Sirlin, Phys. Rev. D22, 2695 (1980); Phys. Rev. D31, 213 (1985); A. Sirlin and W.J. Marciano, Nucl. Phys. B189, 442 (1981); K.I. Aoki et al., Prog. Theor. Phys. Suppl. 73, 1 (1982)
- [20] Particle Data Group, Phys. Lett. B592, 1(2004)
- [21] B.Allanach et al, Phys. Rev. D69, 115002 (2004), Phys. Rev. D60, 075014(1999), hep-ph/9906224; Shaouly Bar-Shalom et al, Phys. Rev. D67, 014007(2003)
- [22] H.Eberl, K.Hidaka *et al.*, Phys. Rev. D62, 055006 (2000) A.Savoy-Navarro, talk at the International Europhysics Conference on High Energy Physics (HEP99), 15-21. July 1999, Tampere, Finland. For transparencies see <http://neutrino.pc.helsinki.fi/hep99/Transparencies/session-07/Savoy-Navarro.pdf>
- [23] Howard E.Haber, SCIPP 93/49 NSF-ITP-94-30,(1994)

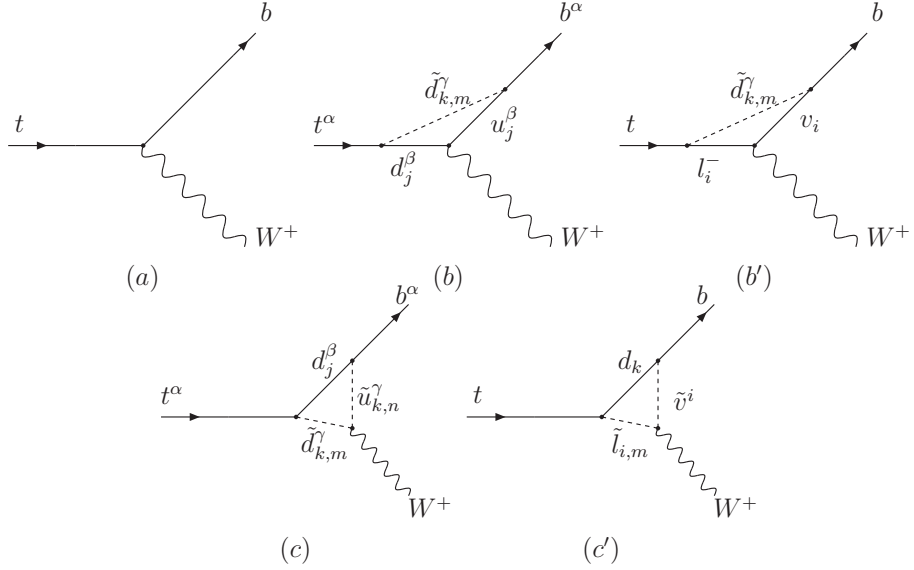


Figure 1: The Feynman diagrams including tree-level and vertex corrections for $t \rightarrow bW^+$.
 (b)((b')) and (c)((c')) are, respectively, for $\lambda''(\lambda')$.

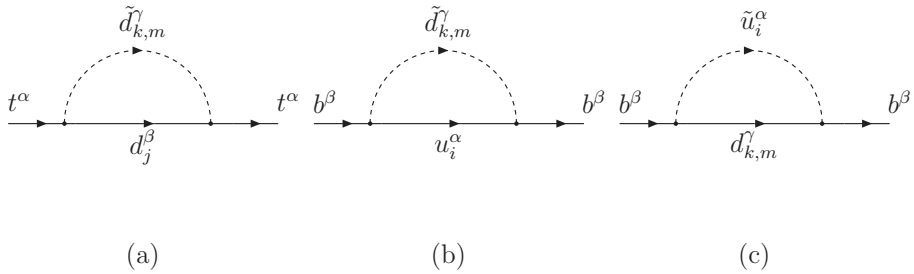


Figure 2: The self-energy diagrams of the top-quark and the bottom quark for λ'' . (a) is for the top quark, (b) and (c) are for the bottom quark.

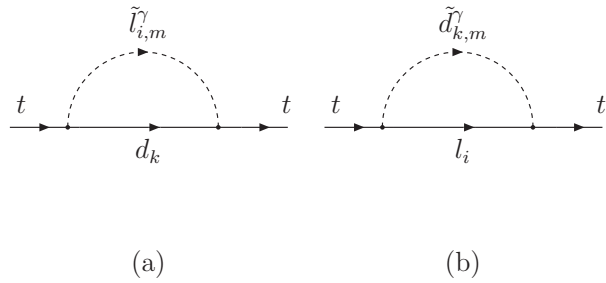


Figure 3: The self-energy diagrams of the top quark for λ' .

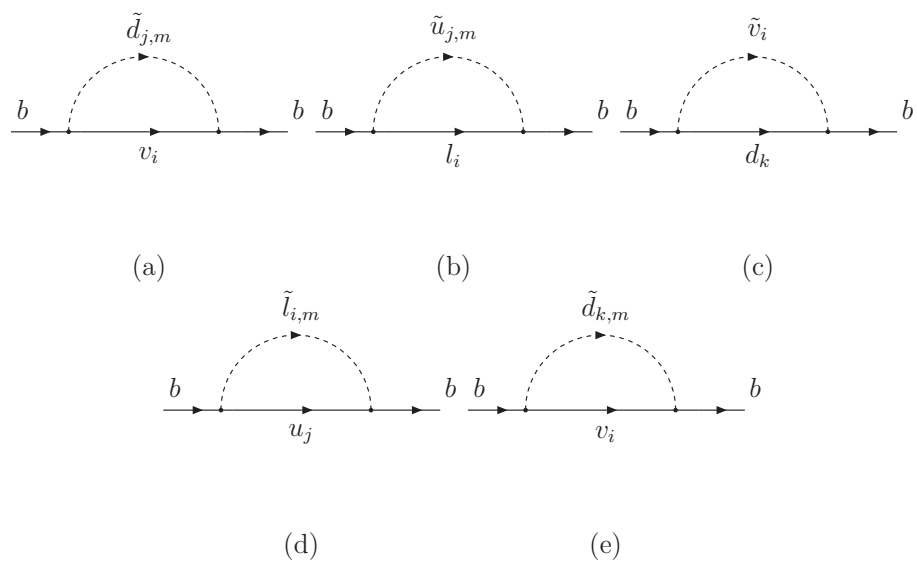


Figure 4: The self-energy diagrams of the bottom quark for λ' .

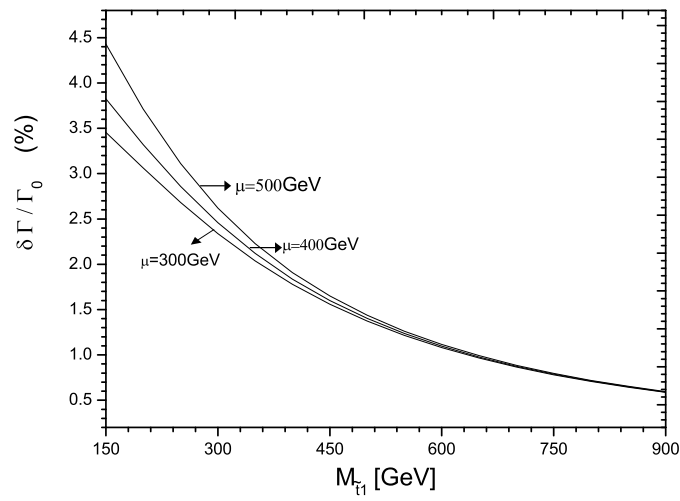


Figure 5: Dependence of the total corrections $\delta\Gamma/\Gamma_0$ on the parameter $m_{\tilde{t}_1}$, assuming $\tan\beta = 40$, $A_t = A_b = 1000\text{GeV}$ and $\mu = 300, 500, 600\text{GeV}$, respectively

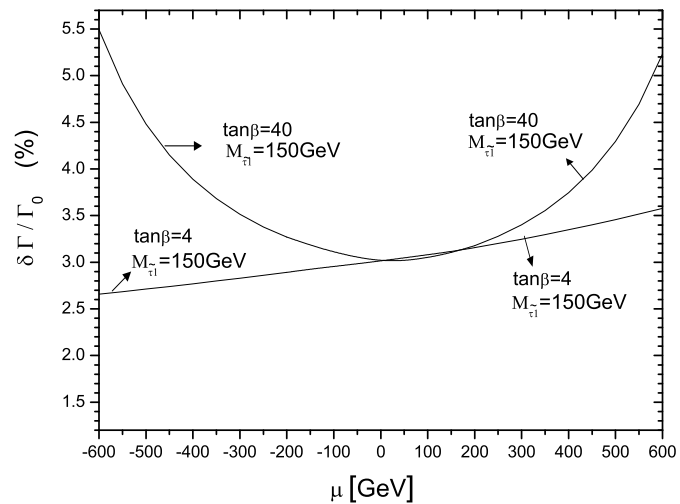


Figure 6: Dependence of the total corrections $\delta\Gamma/\Gamma_0$ on the parameter μ , assuming $m_{\tilde{t}_1} = 150\text{GeV}$, $A_t = A_b = 1000\text{GeV}$ and $\tan\beta = 4, 40$, respectively

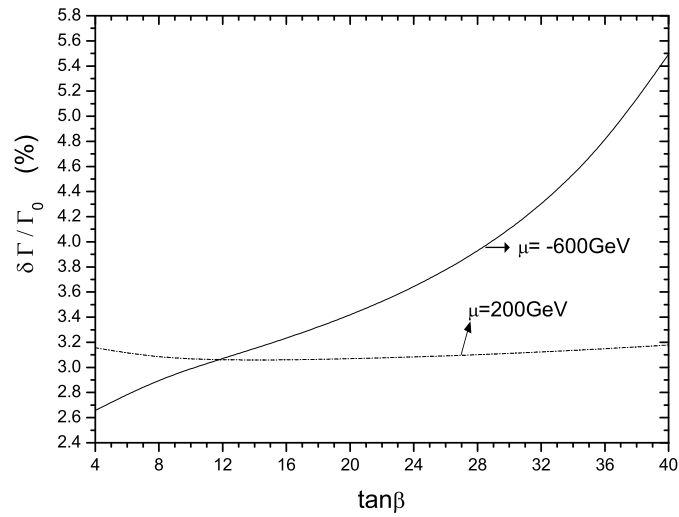


Figure 7: Dependence of the total corrections $\delta\Gamma/\Gamma_0$ on the parameter $\tan\beta$, assuming $m_{\tilde{t}_1} = 150\text{GeV}$, $A_t = A_b = 1000\text{GeV}$ and $\mu = -600, 200\text{GeV}$, respectively

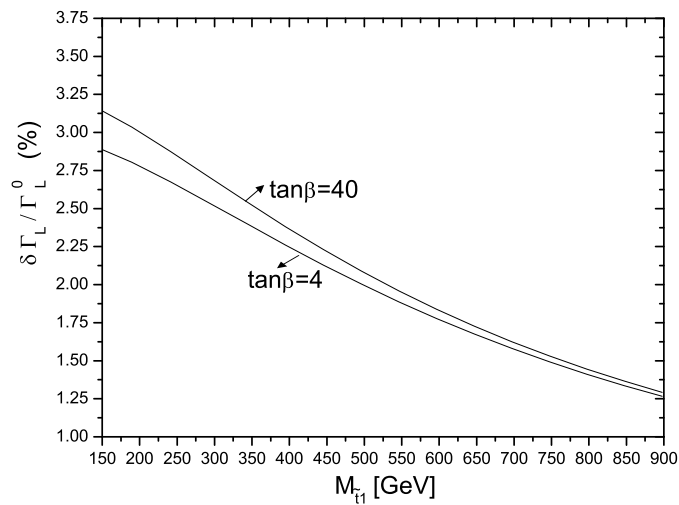


Figure 8: Dependence of the longitudinal corrections $\delta\Gamma/\Gamma_L^0$ on the parameter $m_{\tilde{t}_1}$, assuming $\mu = 300\text{ GeV}$, $A_t = A_b = 1000\text{GeV}$ and $\tan\beta = 4, 40$, respectively

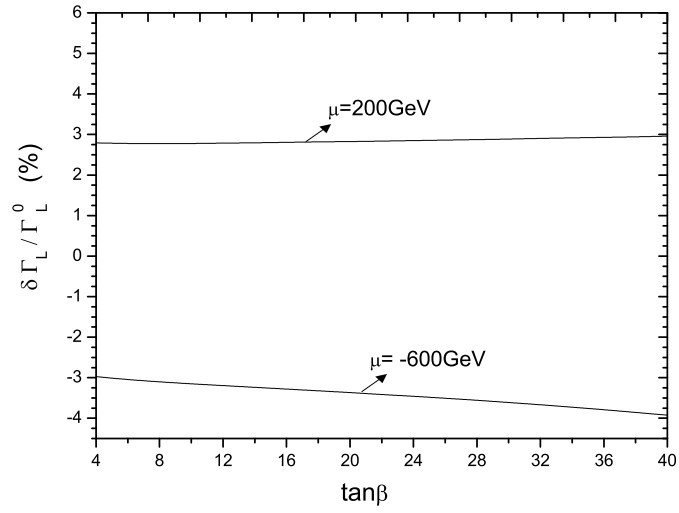


Figure 9: Dependence of the longitudinal corrections $\delta\Gamma_L/\Gamma_L^0$ on the parameter $\tan\beta$, assuming $m_{\tilde{t}_1} = 150\text{GeV}$, $A_t = A_b = 1000\text{GeV}$ and $\mu = -600, 200\text{GeV}$, respectively

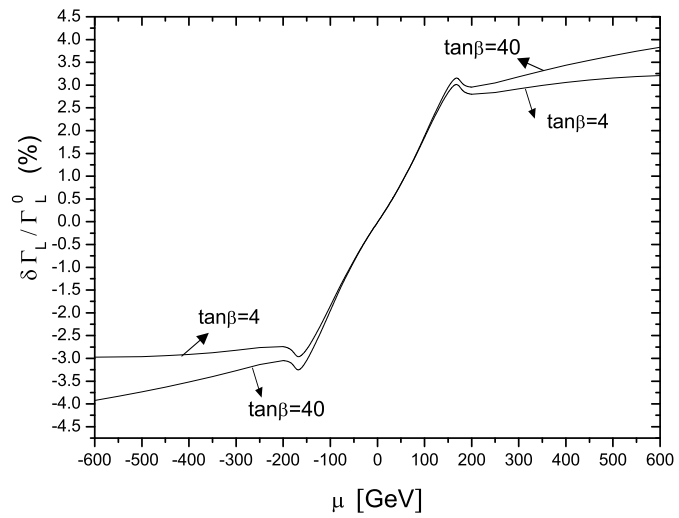


Figure 10: Dependence of the longitudinal corrections $\delta\Gamma_L/\Gamma_L^0$ on the parameter μ , assuming $m_{\tilde{t}_1} = 150\text{GeV}$, $A_t = A_b = 1000\text{GeV}$ and $\tan\beta = 4, 40$.

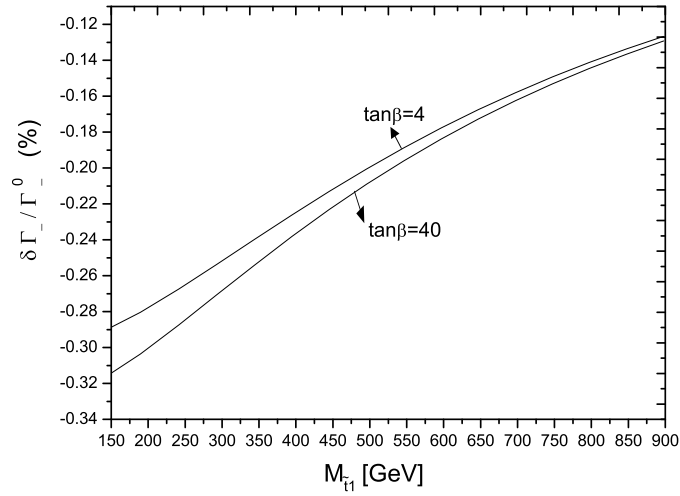


Figure 11: Dependence of the transverse-minus corrections $\delta\Gamma_-/\Gamma_-^0$ on the parameter $m_{\tilde{t}_1}$, assuming $\mu = 300\text{GeV}$, $A_t = A_b = 1000\text{GeV}$ and $\tan\beta = 4, 40$, respectively

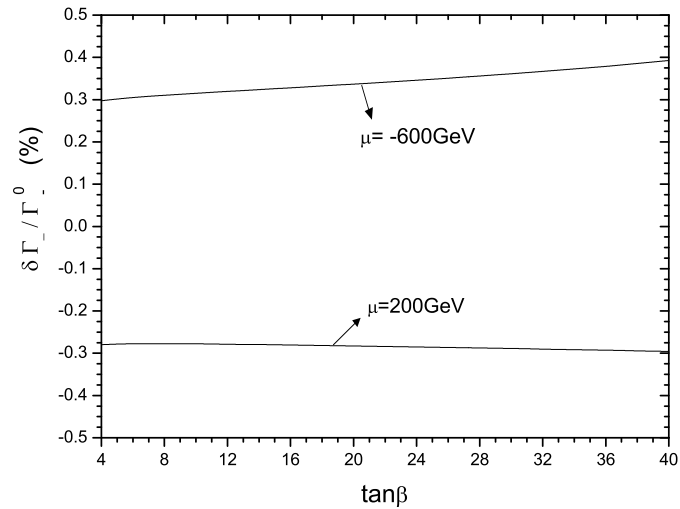


Figure 12: Dependence of the transverse-minus corrections $\delta\Gamma_-/\Gamma_-^0$ on the parameter $\tan\beta$, assuming $m_{\tilde{t}_1} = 150\text{GeV}$, $A_t = A_b = 1000\text{GeV}$ and $\mu = -600, 200\text{GeV}$, respectively

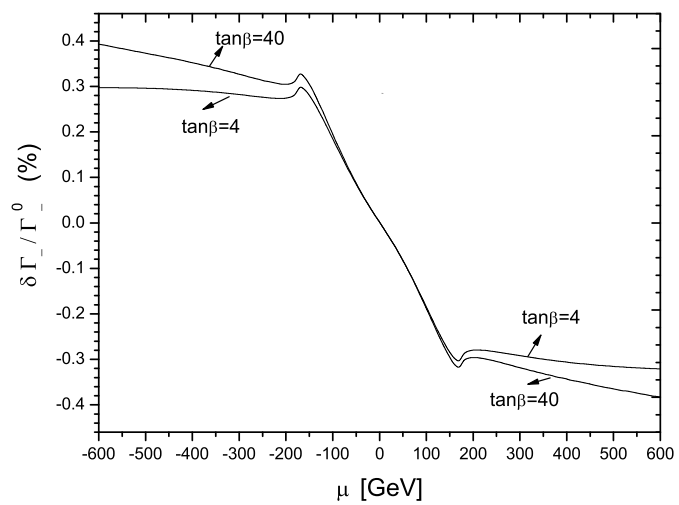


Figure 13: Dependence of the transverse-minus corrections $\delta\Gamma_-/\Gamma_-^0$ on the parameter μ , assuming $m_{\tilde{t}_1} = 150\text{GeV}$, $A_t = A_b = 1000\text{GeV}$ and $\tan\beta = 4, 40$, respectively